논문 15-40-07-01 The Journal of Korean Institute of Communications and Information Sciences '15-07 Vol.40 No.07
http://dx.doi.org/10.7840/kics.2015.40.7.1217

On the Characteristics of MSE-Optimal Symmetric Scalar Quantizers for the Generalized Gamma, Bucklew-Gallagher, and Hui-Neuhoff Sources

Jagan Rhee◆, Sangsin Na°

ABSTRACT

The paper studies characteristics of the minimum mean-square error symmetric scalar quantizers for the generalized gamma, Bucklew-Gallagher and Hui-Neuhoff probability density functions. Toward this goal, asymptotic formulas for the inner- and outermost thresholds, and distortion are derived herein for nonuniform quantizers for the Bucklew-Gallagher and Hui-Neuhoff densities, parallelling the previous studies for the generalized gamma density, and optimal uniform and nonuniform quantizers are designed numerically and their characteristics tabulated for integer rates up to 20 and 16 bits, respectively, except for the Hui-Neuhoff density. The assessed asymptotic formulas are found consistently more accurate as the rate increases, essentially making their asymptotic convergence to true values numerically acceptable at the studied bit range, except for the Hui-Neuhoff density, in which case they are still consistent and suggestive of convergence. Also investigated is the uniqueness problem of the differentiation method for finding optimal step sizes of uniform quantizers: it is observed that, for the commonly studied densities, the distortion has a unique local minimizer, hence showing that the differentiation method yields the optimal step size, but also observed that it leads to multiple solutions to numerous generalized gamma densities.

Key Words : scalar quantization, generalized gamma source, Bucklew-Gallagher source, Hui-Neuhoff source, asymptotic formulas, MSE distortion

Ⅰ. Introduction

Quantization is an integral part of converting an analog signal to a digital form for further processing, communication and/or storage, such as in a GPS system[1], a soft-decision error correction system[2] or a multiple antenna mobile system[3]. In such applications it is important to estimate the performance and key characteristics of quantizers for the system design and performance analysis. In general without actual design it is difficult to estimate accurately thresholds, quantization levels, and the mean-square error (MSE) distortion of an optimal (minimum MSE) quantizer. However, when the number of levels is large, the high resolution quantization theory[4-10] has discovered approximation formulas that are increasingly accurate with more number of levels for some of such characteristics. This paper extends in particular these two studies[9-10], respectively, to nonuniform quantizers and to source probability density functions (pdfs) with heavier tails; investigates the uniqueness problem of the differentiation approach[9] for finding optimal step sizes; and assesses accuracies of these formulas by comparing them with those of numerically designed quantizers.

◆ First Author : Ph.D from Electrical and Computer Engineering, Ajou University, Suwon, Republic of Korea, altitude@ajou.ac.kr, 정회원
° Corresponding Author : Department of Electrical and Computer Engineering, Ajou University, Suwon, Republic of Korea, sangna@ajou.ac.kr, 종신회원
논문번호 : KICS2015-06-166, Received June 2, 2015; Revised July 6, 2015; Accepted July 6, 2015

We focus on symmetric uniform and nonuniform scalar quantizers with even number $N=2K$ of levels that are applied to symmetric pdfs, as illustrated in Fig. 1, where only the nonnegative half of the quantizer is labeled for the sake of simplicity for thresholds $x_1,\cdots,x_K$ with $x_{K+1}=\infty$ and quantization levels $y_1,\cdots,y_K$. The word "symmetric" is sometimes dropped because it is the only type considered, although truly optimal quantizers may not be symmetric.

The (total) MSE distortion D_t of $2K$-level symmetric quantizer applied to a source with symmetric pdf $p(x)$ can be thought to be the sum of distortions from the inner region $[-x_K,x_K]$ and the outer region $(-\infty,-x_K)\cup(x_K,\infty)$. The former will be called the inner distortion D_i and the latter the outer distortion D_o. These correspond essentially to more commonly-known granular and overload distortions, although they are slightly different. Then

$$\begin{aligned} D_t &= 2\sum_{k=1}^{K}\int_{x_k}^{x_{k+1}}(x-y_k)^2 p(x)dx \\ &= \underbrace{2\sum_{k=1}^{K-1}\int_{x_k}^{x_{k+1}}(x-y_k)^2 p(x)dx}_{D_i} + \underbrace{2\int_{x_K}^{\infty}(x-y_K)^2 p(x)dx}_{D_o}. \end{aligned} \quad (1)$$

The primary interest of the paper is the following characteristics of optimal symmetric uniform and nonuniform quantizers: (a) the nonzero innermost threshold x_2 and level y_1 because these are an indicator to how the quantizer treats small input values; (b) the outermost threshold x_K and level y_K because they show how the quantizer treats large input values; and (c) the inner, outer and total distortions D_i, D_o, and D_t, respectively.

The source densities considered for the study are: (a) the generalized gamma pdf as a representative of light-tailed densities, to which the common generalized gamma (the Gaussian, two-sided Rayleigh, Laplacian, and usual gamma) pdfs belong; (b) the Bucklew-Gallagher pdf as a heavy-tailed density; and (c) the Hui-Neuhoff pdf as a very heavy-tailed density.

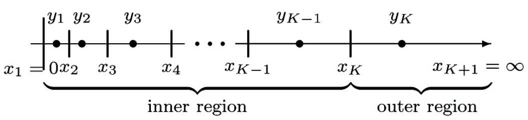

Fig. 1. Nonnegative half of a symmetric scalar quantizer under study

The principal results of the paper include asymptotic formulas for the characteristics that are newly derived herein for nonuniform quantizers for the Bucklew-Gallagher and Hui-Neuhoff pdfs, parallelling those for the generalized gamma pdfs[10]. Overall the formulas are observed to be accurate for the generalized gamma and Bucklew-Gallagher pdfs, for example, in that the percent error of the formulas for x_2 of uniform and nonuniform quantizers is within 1% from true values for rate $R=\log_2 N\geq 12$ bits, whereas, although those for the Hui-Neuhoff pdf are not as accurate at studied rates, they are still suggestive of consistent patterns for convergence. For the accuracy assessment of the formulas, optimal uniform quantizers are numerically designed using direct minimization for integer R up to 20 bits, extended from 16 bits[10], and nonuniform quantizers using the Lloyd-Max algorithm[11-12] up to 16 except for the Hui-Neuhoff pdf, in which case the maximum rate is 11, beyond which the design is a challenge inviting much more care.

Also presented is an investigation on the uniqueness problem of the differentiation method[9] for finding optimal step sizes of uniform quantizers. It is found that, for the four common generalized gamma, Bucklew-Gallagher, and Hui-Neuhoff pdfs, D_t is either convex-U in the step size or non-convex but has a unique local (hence global) minimizer, and therefore the differentiation method yields a unique solution for all of them, but also that there exist numerous generalized gamma pdfs for which the differentiation method leads to multiple solutions, the smallest among which, nevertheless, always seems to be the optimal step size in the case of the studied pdfs.

To the best of the authors' knowledge the formulas for optimal nonuniform quantizers for the Bucklew-Gallagher and Hui-Neuhoff pdfs and the investigation on the uniqueness problem of the differentiation method have not been previously reported in the literature.

The rest of the paper is organized as follows. Section II lists the source pdfs of interest, Section III investigates the uniqueness problem associated with the differentiation method for optimal step sizes, Section IV studies asymptotic formulas for the characteristics of optimal quantizers for various pdfs and assesses accuracies of the formulas comparing them with numerically designed quantizers, and finally Section V concludes.

Ⅱ. The Source Distributions

The probability density function of the generalized gamma (G-Γ) distribution[13] is defined as

$$p(x;\alpha,\beta,\lambda)=\frac{\alpha\lambda^{\frac{\beta+1}{\alpha}}}{2\Gamma\left(\frac{\beta+1}{\alpha}\right)}|x|^{\beta}e^{-\lambda|x|^{\alpha}}\quad, \tag{2}$$

where $\alpha>0$, $\beta>-1$, $\lambda>0$, and $\Gamma(x)=\int_0^{\infty}e^{-t}t^{x-1}dt$ is the gamma function. The G-Γ pdf specializes to the Gaussian $p\left(x;2,0,\frac{1}{2\sigma^2}\right)$, two-sided Rayleigh $p\left(x;2,1,\frac{1}{\sigma^2}\right)$, Laplacian $p\left(x;1,0,\frac{\sqrt{2}}{\sigma}\right)$, and usual gamma $p\left(x;1,-\frac{1}{2},\frac{\sqrt{3}}{2\sigma}\right)$, where σ is the standard deviation. The Bucklew-Gallagher (B-G) pdf[5] is defined as

$$p(x;\delta)=\frac{1+\frac{\delta}{2}}{(1+|x|)^{3+\delta}}\quad, \tag{3}$$

where $\delta>0$. It is symmetric about zero, unimodal, and has unit variance when $\delta=1$. The Hui-Neuhoff (H-N) pdf[7] is defined as

$$p(x;\delta)=\frac{C_\delta}{(|x|+2)^3\left[\ln(|x|+2)\right]^{\delta+1}}\quad, \tag{4}$$

where $\delta>0$, the normalization constant C_δ is given by $C_\delta=\frac{1}{2^{\delta+1}\Gamma(-\delta,\ln 4)}$, where $\Gamma(a,x)=\int_x^{\infty}x^{a-1}e^{-t}dt$ is the complementary incomplete gamma function. It is also symmetric about zero, unimodal, and has the unit variance and $C_\delta=3.46458\cdots$ when $\delta=2.38636\cdots$, all numerically obtained.

The G-Γ pdf has a light tail, the B-G heavy, and the H-N very heavy. For the B-G and the H-N pdfs, a smaller δ implies a heavier tail and a larger variance. The G-Γ and B-G pdfs satisfy Bucklew and Wise's finite moment condition[6] of Thm. 2, i.e., $E[|X|^{2+\epsilon}]<\infty$ for some $\epsilon>0$, but the H-N does not.

Ⅲ. The Uniqueness Problem of the Differentiation Method

The uniform quantizer studied in the paper is specified by $x_k=(k-1)\Delta$ and $y_k=\left(k-\frac{1}{2}\right)\Delta$, $k=1,\cdots K$, where Δ is the step size, the distance between adjacent thresholds, which equals x_2. In such a case, the inner and outer distortions D_i and D_o in (1) reduce respectively to

$$D_i=2\sum_{k=1}^{K-1}\int_{(k-1)\Delta}^{k\Delta}\left\{x-\left(k-\frac{1}{2}\right)\Delta\right\}^2p(x)dx \tag{5}$$

$$D_o=2\int_{(K-1)\Delta}^{\infty}\left\{x-\left(K-\frac{1}{2}\right)\Delta\right\}^2p(x)dx. \tag{6}$$

We now investigate the uniqueness problem of the differentiation method[9] for finding optimal step sizes.

Designing an optimal uniform quantizer is essentially finding optimal Δ that minimizes $D_t=D_i+D_o$. To do so, one would normally try the differentiation method, i.e., solve $\frac{dD_t}{d\Delta}=0$ for Δ. This method, though probably the de facto standard, in general does not yield the optimal step size directly but its candidate(s). However, in the following it is shown that it yields a unique solution in the case of the four common G-Γ, B-G, and H-N pdfs: D_t is convex-U in Δ in all the cases except for the two-sided Rayleigh pdf.

3.1 On the Convexity of D_t

Distortion D_t of a uniform quantizer when applied to a source with symmetric pdf $p(x)$, denoted $D_t(K,\Delta)$ to show its explicit dependence on K and Δ, can be rewritten as, for $K \geq 2$,

$$D_t(K,\Delta) = 2\int_0^\infty x^2 p(x)dx - 2\Delta\int_0^\infty xp(x)dx + \frac{\Delta^2}{4} + 4\Delta\sum_{k=1}^{K-1}\int_{k\Delta}^\infty (k\Delta - x)p(x)dx \quad (7)$$

after rearrangement of integration intervals in the summation in (5) and some manipulation, which yields the following first and second derivatives with respect to Δ:

$$D_t'(K,\Delta) = -2\int_0^\infty xp(x) + \frac{\Delta}{2} + 4\sum_{k=1}^{K-1}\int_{k\Delta}^\infty (2k\Delta - x)p(x)dx, \quad (8)$$

$$D_t''(K,\Delta) = \frac{1}{2} + 4\sum_{k=1}^{K-1}\left\{2k\int_{k\Delta}^\infty p(x)dx - k^2\Delta p(k\Delta)\right\}. \quad (9)$$

In the case of $K=1$, there are no summation terms in (7)-(9).

As noted[9], since $\lim_{\Delta\to 0^+} D_t(K,\Delta) = \sigma^2$, $\lim_{\Delta\to 0^+} D_t'(K,\Delta) < 0$, and $\lim_{\Delta\to\infty} D_t(K,\Delta) = \infty$, $D_t(K,\Delta)$ achieves its global minimum in $(0,\infty)$. Furthermore, if it is convex-U in Δ, the global minimum is achieved at its unique local minimizer Δ^*, which can be found by solving $D_t'(K,\Delta) = 0$ for Δ. A sufficient condition for the U-convexity is a positive second derivative, i.e., $D_t''(K,\Delta) > 0$ for $\Delta > 0$. Behaviors of $D_t''(K,\Delta)$ for several values of K are shown in Figs. 2 and 3 as representative pdfs, where only relatively small values of K are chosen for the plotting purpose. In general, for any pdf $D_t''(1,\Delta) = \frac{1}{2}$, and, as K increases, $D_t''(K,\Delta)$ develops a better-defined knee that forms at a smaller Δ with the knee level approaching $\frac{1}{6}$. Its behavior depending on a specific pdf can be classified into two cases, as discussed in the following.

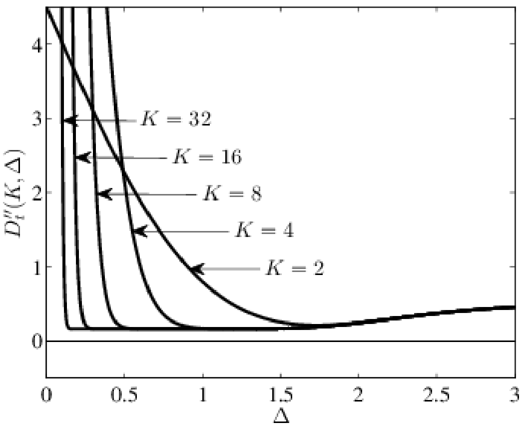

Fig. 2. Behavior of $D_t''(K,\Delta)$ for the unit-variance Gaussian pdf

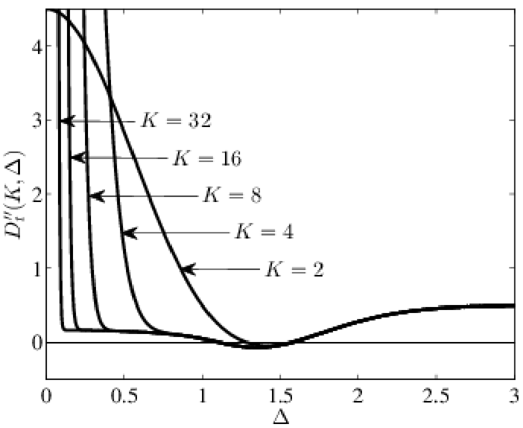

Fig. 3. Behavior of $D_t''(K,\Delta)$ for the unit-variance two-sided Rayleigh pdf

One case is when $D_t''(K,\Delta) > 0$ for each $K \geq 2$, exhibiting that $D_t(K,\Delta)$ is convex-U for each K. All the previously mentioned pdfs except for the two-sided Rayleigh belong to this case, including the Gaussian shown in Fig. 2. Based on extensive observations (for $K = 2,\cdots,2000$ and much larger 2^{20} in some cases), it is conjectured that in order to check for the positiveness of $D_t''(K,\Delta)$ for all $K \geq 2$, it is sufficient to check if $\min_\Delta D_t''(2,\Delta)$ is positive. The reason is that, once $D_t''(2,\Delta) > 0$,

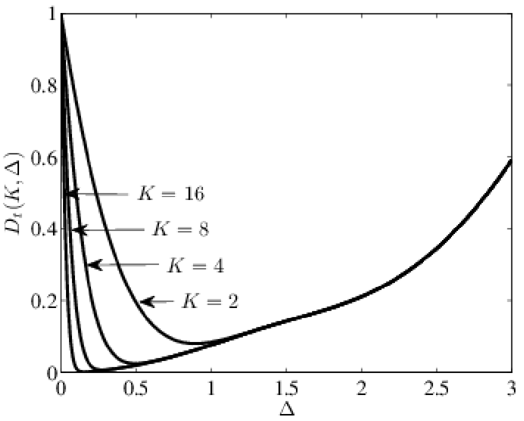

Fig. 4. Behavior of $D_t(K,\Delta)$ for the unit-variance two-sided Rayleigh pdf

then it appears that $D_t''(K,\Delta)$ does not fall below zero as K increases.

Another case is represented by the two-sided Rayleigh pdf, for which Fig. 3 shows the minimum of $D_t''(K,\Delta)$ is negative around $\Delta=\sqrt{2}$ (exactly if $K=2$), implying the nonconvexity of $D_t(K,\Delta)$. However, $D_t'(K,\Delta)=0$ has a unique solution, as can be inferred from Fig. 4, which shows how $D_t(K,\Delta)$ behaves with Δ.

3.2 Further Investigation in the Case of G-Γ PDFs

Upon accepting the conjecture that $\min_\Delta D_t''(2,\Delta)>0$ implies the convexity of $D_t(K,\Delta)$ for $K=3,4,\cdots$, the unit-variance G-Γ pdfs can be classified into three groups: those for which $D_t(K,\Delta)$ is convex-U and hence has a unique global minimum; those for which it is not convex but has a unique local (hence global) minimum; and the rest for which it has multiple local minima. Fig. 5 shows the three regions defined by these groups, where the thin-lined boundary between the convex and the unioptimum regions is determined by the set of (α,β) that satisfies numerically $\min_\Delta D_t''(2,\Delta)=0$, that is Eq. (9) with $K=2$ evaluated at its minimizer $\Delta=\left\{\frac{\beta+3}{\alpha}\right\}^{\frac{1}{\alpha}}\left\{\frac{\Gamma((\beta+1)/\alpha)}{\Gamma((\beta+3)/\alpha)}\right\}^{\frac{1}{2}}$ and set to 0, and the other boundary, thick-lined, by the set of (α,β) for which $D_t'(2,\Delta)=0$ has (numerically observed) multiple solutions. Also shown in Fig. 5 are the locations of the Gaussian G, Laplacian L, usual gamma Γ pdfs belonging to the convex region; and the two-sided Rayleigh R to the unioptimum region. Point $A(2,3)$ is particularly notable as an example of pdfs in the multiextrema region and the behavior of its $D_t(K,\Delta)$ is shown in Fig. 6, which clearly shows multiple (two in this case) local minima for $K\geq 2$, between which the smaller is the global minimum. Although details are not given in the paper, it is noted that the number of local minima increases as α and β increase, e.g., three local minima are observed for $B(6,6)$, among which the global minimum is achieved at the smallest local minimizer. As a comment we add that the convex region is of course a subset of the unioptimum region and we find it more convenient to check the

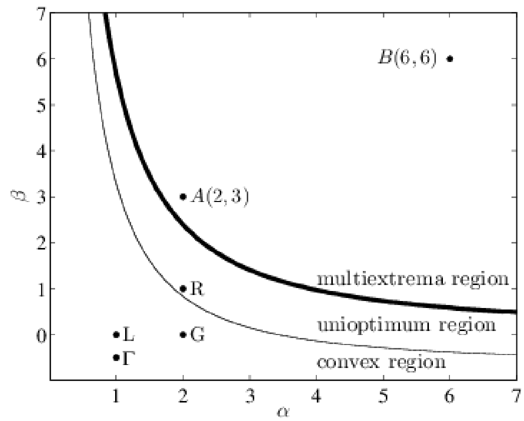

Fig. 5. Three regions for the unit-variance G-Γ pdfs

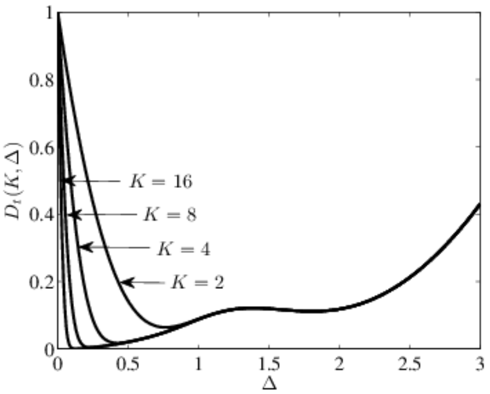

Fig. 6. Behavior of $D_t(K,\Delta)$ for unit-variance G-Γ pdf with $\alpha=2$ and $\beta=3$

convexity, if that is the case, than the unioptimality because it requires less numerical search efforts.

Ⅳ. Characteristics of Optimal Quantizers

As mentioned in Section I, we focus on such characteristics as x_2 and y_1, x_K and y_K, and D_i, D_o and D_t. We follow the developed methodology[10] and summarize it below.

In the case of optimal N-level uniform quantizers Q_N^U, we use the approach by Hui and Neuhoff[7] for characterizing the asymptotic form of the outermost threshold x_K, from which optimal step size $\Delta(=x_2)$ can be obtained from $\Delta=\frac{x_K}{K-1}$ and $y_1=\frac{\Delta}{2}$. The formulas given in this section for the G-Γ pdf come directly from the previous studies[7,9,10]; the formulas for the B-G and H-N densities are rederived[9] for additional terms.

Asymptotic formulas for distortions of Q_N^U are derived from the expressions[9] in Thm. 4: $D_t = D(Q_N^U) = D_i(Q_N^U) + D_o(Q_N^U)$, where

$$D_i(Q_N^U) = \frac{\Delta^2}{12} + \int_0^{x_2}\left\{2u^2 - 2u\Delta + \frac{\Delta^2}{3}\right\}p(u)du + R_d, \tag{10}$$

$$D_o(Q_N^U) = 2\int_{x_K}^{\infty}u^2p(u)du - 4\left(x_K+\frac{\Delta}{2}\right)\int_{x_K}^{\infty}up(u)du + 2\left(x_K^2 + x_K\Delta + \frac{\Delta^2}{6}\right)\int_{x_K}^{\infty}p(u)du, \tag{11}$$

where $|R_d| \le \frac{(2-2^{-3})\Delta^4}{180}\int_{x_2}^{x_K}|p^{(2)}(u)|du$.

For optimal nonuniform quantizer Q_N^*, we use the formula from the previous study[8] for x_K for the G-Γ, and derive new formulas for the B-G and H-N pdfs. An expression for optimal x_2 can be heuristically found in terms of N by following, e.g., the differentiation method[8]: solve $\frac{dD(Q_N)}{dx_2}=0$ for x_2, where $D(Q_N)$, i.e., D_t in (1), in order to show the dependence on x_2 explicitly, is rewritten as

$$D(Q_N) = 2\left[\int_0^{x_2}(x-y_1)^2p(x)dx + \int_{x_2}^{\infty}(x-Q_N(x))^2p(x)dx\right]$$

where y_1 is the optimal level of $[0,x_2)$, i.e.,

$$y_1 = \frac{\int_0^{x_2}xp(x)dx}{\int_0^{x_2}p(x)dx}. \tag{12}$$

When the second integration term in the bracket is approximated as a Panter-Dite formula-like expression[4] for optimal Q_N^*, we have

$$D(Q_N^*) \approx 2\int_0^{x_2}(x-y_1)^2p(x)dx + \frac{1}{12N^2}\left(2\int_{x_2}^{\infty}p^{1/3}(x)dx\right)^3.$$

This approach is heuristic because, instead of the derivative of the original $D(Q_N)$, that of the right hand side of the above approximation expression is used. For a specific $p(x)$, since y_1 is given in (12), x_2 is the only unknown in $\frac{dD(Q_N^*)}{dx_2}=0$, which reduces to

$$(x_2-y_1)p^{1/3}(x_x) - \frac{1}{N}\int_{x_2}^{\infty}p^{1/3}(x)dx = 0, \tag{13}$$

from which x_2 can be found.

An asymptotic formula for $D_i(Q_N^*)$, i.e., D_i in (1), is provided by the Panter-Dite formula[4]

$$D_i(Q_N^*) = \frac{1}{12N^2}\left(2\int_0^{x_K}p^{1/3}(x)dx\right)^3(1+o_N(1)), \tag{14}$$

where the "little o" $o_N(1)$ denotes a quantity that vanishes as $N\to\infty$, i.e., $\lim_{N\to\infty}o_N(1)=0$.

An asymptotic expression for $D_o(Q_N^*)$, i.e., D_o in (1), is obtained using the formula for optimal x_K and noting that y_K is the optimal level of $[x_K,\infty)$, i.e.,

$$y_k = \frac{\int_{x_K}^{\infty}xp(x)dx}{\int_{x_K}^{\infty}p(x)dx}. \tag{15}$$

Specific formulas for these characteristics are given and discussed in the subsections that follow.

To assess the accuracies of the formulas, optimal symmetric quantizers are designed and their characteristics are tabulated in Tables 3-8: uniform quantizers with integer rate R up to 20 bits are designed with direct minimization (so the rate is extended from 16 in the case of the common G-Γ pdfs[10]); and nonuniform quantizers with up to 16 bits for the B-G pdf with the Lloyd-Max algorithm[11-12] and for the Hui-Neuhoff pdf up to 11 bits, beyond which the design has experienced a numerical challenge. Overall the designed quantizers agree with those[7] to the extent reported.

4.1 The G-Γ PDFs

4.1.1 Optimal Uniform Quantizers Q_N^U

The optimal outermost threshold x_K for the G-Γ pdf is found following the method of the previous papers[7,9] and using the binomial series of $(1+u)^r = 1 + ru + \cdots$ for $|u| < 1$ and is quoted[10] to be:

$$x_K \approx \left(\frac{2\ln N}{\lambda}\right)^{\frac{1}{\alpha}} \left(1 + \frac{c_1 \ln\ln N}{\alpha \ln N} + \frac{c_2}{\alpha \ln N} + \frac{(1-\alpha)\, c_1^2 (\ln\ln N)^2}{2\alpha^2 (\ln N)^2} + \left(\frac{c_1^2}{\alpha} + \frac{(1-\alpha) c_1 c_2}{\alpha^2}\right) \frac{\ln\ln N}{(\ln N)^2}\right),$$

where

$$c_1 = -\frac{2\alpha - \beta - 1}{2\alpha},\ \ c_2 = -\frac{1}{2} \ln\left\{\frac{2^{\frac{2\alpha-\beta-1}{\alpha}} \alpha \Gamma\left(\frac{\beta+1}{\alpha}\right)}{3}\right\}.$$

Formulas for other quantities are obtained using the above expression for x_K. For example, $x_2 (= \Delta)$ is found from $x_K = (K-1)x_2$ or

$$x_2 \approx \frac{2}{N}\left(\frac{2\ln N}{\lambda}\right)^{\frac{1}{\alpha}} \left(1 + \frac{c_1}{\alpha}\frac{\ln\ln N}{\ln N} + \frac{c_2}{\alpha}\frac{1}{\ln N} + \frac{(1-\alpha)c_1^2}{2\alpha^2}\frac{(\ln\ln N)^2}{(\ln N)^2} + \left(\frac{c_1^2}{\alpha} + \frac{(1-\alpha)c_1 c_2}{\alpha^2}\right)\frac{\ln\ln N}{(\ln N)^2}\right)$$

and distortion formulas (quoted from the work[10]):

$$D_i(Q_N^U) \approx \frac{1}{3}\left(\frac{2}{\lambda}\right)^{\frac{2}{\alpha}} \frac{(\ln N)^{\frac{2}{\alpha}}}{N^2}\left\{1 - \frac{2\alpha-\beta-1}{\alpha^2}\frac{\ln\ln N}{\ln N}\right\},$$

$$D_o(Q_N^U) \approx \frac{1}{3\alpha}\left(\frac{2}{\lambda}\right)^{\frac{2+\alpha}{\alpha}} \frac{(\ln N)^{\frac{2-\alpha}{\alpha}}}{N^2},$$

$$D(Q_N^U) \approx \frac{C_{HN}(\ln N)^{2/\alpha}}{N^2}\left\{1 + \frac{2c_1}{\alpha}\frac{\ln\ln N}{\ln N}\right\},$$

where the Hui-Neuhoff asymptotic constant C_{HN} is defined as

$$C_{HN} = \lim_{N\to\infty} \frac{N^2 D(Q_N^U)}{(\ln N)^{2/\alpha}} = \frac{2^{2/\alpha}\Gamma\left(\frac{\beta+1}{\alpha}\right)}{3\Gamma\left(\frac{\beta+3}{\alpha}\right)}\sigma^2$$

after their discovery[7].

Assuming the accuracy of the distortion formulas, one can see that, as the ratio $\frac{D_o(Q_N^U)}{D_i(Q_N^U)} \approx \frac{1}{\alpha \ln N}$ indicates, the inner distortion dominates the outer distortion in the case of the optimal uniform quantizer for the G-Γ source.

4.1.2 Optimal Nonuniform Quantizers Q_N^*

For a symmetric quantizer Q_N^* optimized for the G-Γ pdf, the outermost threshold x_K is found and reported[8] as:

$$x_K \approx \left(\frac{3\ln N}{\lambda}\right)^{\frac{1}{\alpha}}\left\{1 - \frac{3\alpha-\beta-3}{3\alpha^2}\frac{\ln\ln N}{\ln N} + \frac{\ln\left(3\Gamma\left(\frac{\beta+3}{3\alpha}\right)\right)}{\alpha}\frac{1}{\ln N}\right\}.$$

Then from (15)

$$y_K = \frac{\Gamma\left(\frac{\beta+2}{\alpha}, \lambda x_K^\alpha\right)}{\lambda^{1/\alpha}\Gamma\left(\frac{\beta+1}{\alpha}, \lambda x_K^\alpha\right)} = x_K\left\{1 + \frac{1}{\alpha\lambda}\frac{1}{x_K^\alpha} + O\left(\frac{1}{x_K^{2\alpha}}\right)\right\}$$

using the asymptotic expansion[14]: $z \to \infty$

$$\Gamma(a,z) = e^{-z} z^{a-1}\left\{1 + \frac{a-1}{a} + O\left(\frac{1}{z^2}\right)\right\}, \qquad (16)$$

where the "big O" $O(f(x_K))$ denotes a quantity "bounded" by $f(x_K)$, that is there exists a number $M > 0$ such that the quantity is bounded by $M|f(x_K)|$ for all positive integer K. Other "big O" notations are used in similar manners.

For optimal x_2, we use the expression for y_1 from (12)

$$y_1 = \frac{\gamma\left(\frac{\beta+2}{\alpha}, \lambda x_2^\alpha\right)}{\lambda^{1/\alpha}\gamma\left(\frac{\beta+1}{\alpha}, \lambda x_2^\alpha\right)} = \frac{\beta+1}{\beta+2}x_2\left\{1 - \frac{\alpha\lambda x_2^\alpha}{(\alpha+\beta+1)(\alpha+\beta+2)} + O(x_2^{2\alpha})\right\},$$

where $\gamma(a,z)=\int_0^z x^{a-1}e^{-x}dx$ is the incomplete gamma function with convergent series $\gamma(a,z)=z^a\sum_{s=0}^{\infty}(-1)^s\frac{z^s}{s!(a+s)}$, and solve (13) to obtain

$$x_2=\left(\frac{2}{N}\right)^{\frac{3}{\beta+3}}\left(\frac{3}{\lambda}\right)^{\frac{1}{\alpha}}\left\{\frac{\beta+2}{2\alpha}\Gamma\left(\frac{\beta+3}{3\alpha}\right)\right\}^{\frac{3}{\beta+3}}$$
$$\times\left\{1+O\left(\frac{1}{N^{\min(1,\frac{3\alpha}{\beta+3})}}\right)\right\}.$$

Distortion expressions resulting from these are found[10] to be:

$$D_i(Q_N^*)\approx\frac{3^{(\beta-\alpha+3)/\alpha}}{\alpha^2\lambda^{2/\alpha}}\frac{\Gamma^3\left(\frac{\beta+3}{3\alpha}\right)}{\Gamma\left(\frac{\beta+1}{\alpha}\right)}\frac{1}{N^2},$$

$$D_o(Q_N^*)\approx\frac{3^{(\beta+3)/\alpha}}{\alpha^2\lambda^{2/\alpha}}\frac{\Gamma^3\left(\frac{\beta+3}{3\alpha}\right)}{\Gamma\left(\frac{\beta+1}{\alpha}\right)}\frac{1}{N^3},$$

$$D(Q_N^*)\approx\frac{C_{PD}}{N^2},$$

where the Panter-Dite asymptotic constant C_{PD} for the G-Γ pdf is given by

$$C_{PD}=\lim_{N\to\infty}N^2D(Q_N^*)=\frac{3^{(\beta-\alpha+3)/\alpha}}{\alpha^2}\frac{\Gamma^3\left(\frac{\beta+3}{3\alpha}\right)}{\Gamma\left(\frac{\beta+3}{\alpha}\right)}\sigma^2.$$

As in the case of uniform quantizers, the ratio $\frac{D_o(Q_N^*)}{D_i(Q_N^*)}\approx\frac{3}{N}$ indicates that the inner distortion dominates the outer distortion in the case of the G-Γ source.

4.1.3 Numerical Results and Discussion

Figs. 7-9 show the percent errors of the asymptotic formulas for x_2, x_K and $D(Q_N)$ for the common unit-variance G-Γ pdfs from the values in Tables 3-6. In general they estimate the true values with increasing accuracy with the rate.

At $R=10$ the formulas estimate x_2 and x_K within 0.5% error except Q_N^U for the usual gamma pdf, in which case the percent error is 1.42%. At $R=12$ they are all within 0.8%.

At $R=10$ the formulas for $D(Q_N)$ are within 2.5% error except for Q_N^U for the usual gamma pdf,

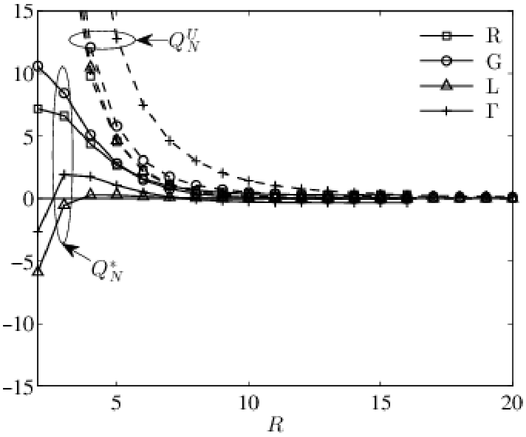

Fig. 7. Percent errors of x_2^U and x_2^* for the common G-Γ pdfs.

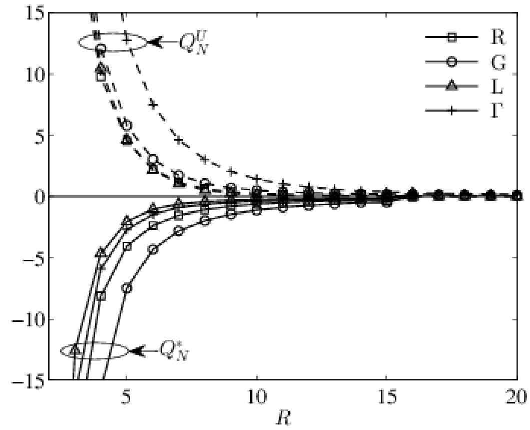

Fig. 8. Percent errors of x_K^U and x_K^* for the common G-Γ pdfs

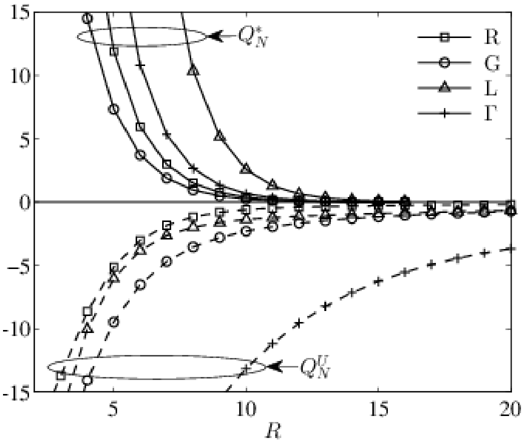

Fig. 9. Percent errors of the asymptotic formulas for $D(Q_N^U)$ and $D(Q_N^*)$ for the common G-Γ pdfs

in which case the percent error is approximately -13%. At $R=16$ they are approximately within 1% except Q_N^U for the usual gamma pdf, in which case the percent error is approximately -5.5%.

Based on these observations, we conclude cautiously that the asymptotic formulas are accurate for the pdfs under study with the exception of those for uniform quantizers for the usual gamma pdf.

4.2 The B-G PDFs

4.2.1 Optimal Uniform Quantizers

For a uniform quantizer Q_N^U optimized for the B-G pdf with parameter δ, the outermost threshold x_K satisfies[7]

$$x_K = \left(\frac{3}{1+\delta}\right)^{\frac{1}{2+\delta}} N^{\frac{2}{2+\delta}} \times \left\{1 - \frac{1+\delta}{2+\delta}\left(\frac{1+\delta}{3}\right)^{\frac{1}{2+\delta}} \frac{1}{N^{2/(2+\delta)}} + O\left(\frac{1}{N^{\min\left(\frac{4}{2+\delta},1\right)}}\right)\right\}. \quad (17)$$

Then, from $x_K=(K-1)\Delta$, we also have

$$x_2 = \Delta = 2\left(\frac{3}{1+\delta}\right)^{\frac{1}{2+\delta}} \frac{1}{N^{\delta/(2+\delta)}} \times \left\{1 - \frac{1+\delta}{2+\delta}\left(\frac{1+\delta}{3}\right)^{\frac{1}{2+\delta}} \frac{1}{N^{2/(2+\delta)}} + O\left(\frac{1}{N^{\min\left(\frac{4}{2+\delta},1\right)}}\right)\right\}. \quad (18)$$

For distortion $D(Q_N^U)$ for the B-G pdf $p(x)$ with parameter δ, we have[9]

$$D(Q_N^U) = D_i(Q_N^U) + D_o(Q_N^U),$$

where

$$D_i(Q_N^U) = \frac{\Delta^2}{12}(1+O(\Delta^2)), \quad (19)$$

$$D_o(Q_N^U) = \frac{2}{\delta(1+\delta)} \frac{1}{(1+x_K)^\delta}\left(1+O\left(\frac{1}{K}\right)\right) \quad (20)$$

as $\Delta \to \infty$ and $K \to \infty$, where the outermost threshold $x_K=(K-1)\Delta$. Then substituting (17) and (18) for x_K and Δ, respectively, in (19) and (20) and manipulating terms yield

$$D_i(Q_N^U) = \left(\frac{1}{3^\delta(1+\delta)^2}\right)^{\frac{1}{2+\delta}} \frac{1}{N^{2\delta/(2+\delta)}}\left\{1+O\left(\frac{1}{N^{\frac{\min(2\delta,2)}{2+\delta}}}\right)\right\},$$

$$D_o(Q_N^U) = \frac{2}{\delta}\left(\frac{1}{3^\delta(1+\delta)^2}\right)^{\frac{1}{2+\delta}} \frac{1}{N^{2\delta/(2+\delta)}}\left\{1+O\left(\frac{1}{N^{\frac{2}{2+\delta}}}\right)\right\}$$

from which we obtain the following asymptotic expression:

$$D(Q_N^U) = \left(1+\frac{2}{\delta}\right)\left(\frac{1}{3^\delta(1+\delta)^2}\right)^{\frac{1}{2+\delta}} \times \frac{1}{N^{2\delta/(2+\delta)}}\left\{1+O\left(\frac{1}{N^{\frac{\min(2\delta,2)}{2+\delta}}}\right)\right\}.$$

As reported already[7,9], D_i and D_o are of the same order in N and neither dominates. Asymptotic formulas corresponding to the unit variance are obtained with $\delta=1$ and listed in Table 1, where the Hui-Neuhoff asymptotic constant $C_{HN} = 3\left(\frac{1}{12}\right)^{\frac{1}{3}} = \left(\frac{3}{2}\right)^{\frac{2}{3}} = 1.3103\cdots$.

4.2.2 Optimal Nonuniform Quantizers

For a nonuniform quantizer Q_N^* optimized for the B-G density with parameter δ, the outermost threshold x_K and threshold x_2 are derived following the procedure described at the beginning of this section:

$$x_K = \left(\frac{\delta}{3(1+\delta)}\right)^{\frac{3}{\delta}} N^{\frac{3}{\delta}}\left\{1+\frac{3(1+\delta)}{\delta}\frac{1}{N}\right\}^{\frac{3}{\delta}},$$

$$x_2 = \frac{6}{\delta}\frac{1}{N}\left\{1-\frac{\delta+3}{\delta}\frac{1}{N}+O\left(\frac{1}{N^2}\right)\right\}.$$

It is straightforward to obtain $y_K = \frac{(2+\delta)x_K+1}{\delta+1}$ from (15). These x_K and y_K yield formulas for $D_i(Q_N^*)$ and $D_o(Q_N^*)$ from (14) and (1), respectively:

$$D_i(Q_N^*) = \frac{9(\delta+2)}{\delta^3}\frac{1}{N^2}\{1+o_N(1)\},$$

$$D_o(Q_N^*) = \frac{3^3(\delta+1)(\delta+2)}{\delta^4}\frac{1}{N^3}\{1+o_N(1)\}.$$

Unlike the uniform case, the ratio D_i/D_o from the above expressions is in the order of N, exhibiting a strong dominance of D_i. The Panter-Dite asymptotic constant is

$C_{PD}=\frac{9(\delta+2)}{\delta^3}=27$ for the unit-variance B-G pdf.

4.2.3 Numerical Results and Discussion

Fig. 10 shows the characteristics of Q_N^U and Q_N^* for the unit-variance B-G pdf and their corresponding asymptotic formulas listed in Table 1. The two sets of increasing graphs on the left subfigure are for x_K: it is observed that the true value x_K^U is 1.00 at $R=2$ and increases exponentially to 11,813 at $R=20$ and the asymptotic formula is approximately within 1% or less from the true values at $R=11$ or larger (the logarithmic values are much closer as shown in the figure), whereas the true value x_K^* is 1.732 at $R=2$ and increases more rapidly and exponentially to 1.486×10^{12} at $R=16$, and its formula underpredicts the values approximately by 13% from $R=7$ to 16 but its logarithmic values are approximately 1% from those of the true values over $R=5$ to 16, as reflected on the two virtually overlapping curves. The decreasing graphs at the bottom are for the values of x_2^U and x_2^* and their asymptotic formulas. The two formulas predict the true values with less than 2% error at $R=9$ or larger.

The right subfigure compares the distortions and asymptotic constants. It is observed that $N^{2/3}D(Q_N^U)$ rapidly converges to $C_{HN}=1.3103$, reaching it within 1% for $R\geq 4$ and $N^2D(Q_N^*)$ to $C_{PD}=27$ within 2% at $R=9$ and 1% at $R\geq 10$. The rapid convergence of $D(Q_N^U)$ is a pleasant surprise considering the situation of the G-Γ pdfs in the previous subsection. The pattern of convergence of $D(Q_N^*)$ is consistent with those of the G-Γ pdfs.

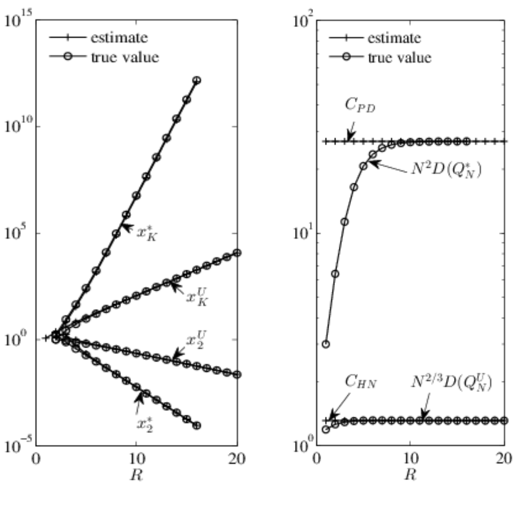

Fig. 10. Characteristics of Q_N^U and Q_N^* and their asymptotes for the unit-variance B-G pdf

Table 1. Asymptotic formulas for optimal quantizer for the unit-variance B-G pdf

Q_N^U	x_2^U	$2\left(\frac{3}{2}\right)^{1/3}\frac{1}{N^{1/3}}\left(1-\left(\frac{2}{3}\right)^{4/3}\frac{1}{N^{2/3}}\right)$
	x_K^U	$\left(\frac{3}{2}\right)^{1/3}N^{2/3}\left(1-\left(\frac{2}{3}\right)^{4/3}\frac{1}{N^{2/3}}\right)$
	$D_i(Q_N^U)$	$\left(\frac{1}{12}\right)^{1/3}\frac{1}{N^{2/3}}$
	$D_o(Q_N^U)$	$2\left(\frac{1}{12}\right)^{1/3}\frac{1}{N^{2/3}}$
	$D(Q_N^U)$	$\frac{C_{HN}}{N^{2/3}};\ C_{HN}=3\left(\frac{1}{12}\right)^{1/3}=1.3103$
Q_N^*	x_2^*	$\frac{6}{N}\left(1-\frac{4}{N}\right)$
	x_K^*	$\left(\frac{N}{6}\right)^3\left(1+\frac{6}{N}\right)^3$
	$D_i(Q_N^*)$	$\frac{27}{N^2}$
	$D_o(Q_N^*)$	$\frac{162}{N^3}$
	$D(Q_N^*)$	$\frac{C_{PD}}{N^2};\ C_{PD}=27$

We conclude that for the B-G pdf

$$D(Q_N^U)\approx\frac{C_{HN}}{N^{2/3}}\quad\text{for } R\geq 4,$$

$$D(Q_N^*)\approx\frac{C_{PD}}{N^2}\quad\text{for } R\geq 10.$$

4.3 The H-N PDFs

For the reason of technicality we assume throughout this subsection the H-N pdf has $\delta>2$ so that the Panter-Dite asymptotic constant exists and is finite. The unit-variance H-N pdf ($\delta=2.38636\cdots$) satisfies this assumption.

4.3.1 Optimal Uniform Quantizers

For a uniform quantizer Q_N^U optimized for the H-N pdf with parameter δ, the outermost threshold

x_K satisfies[7]

$$x_K=\frac{\sqrt{3C_\delta}\,N}{(\ln N)^{(1+\delta)/2}}\left\{1+\left(\frac{1+\delta}{2}\right)^2\frac{\ln\ln N}{\ln N}+O\left(\frac{1}{\ln N}\right)\right\},$$

where $C_\delta=\frac{1}{2^{\delta+1}\Gamma(-\delta,2\ln 2)}=3.46458\cdots$ when $\delta=2.38636\cdots$. Then the resulting D_i and D_o are found[9] to be

$$D_i(Q_N^U)=\frac{\Delta^2}{12}(1+O(\Delta))$$

$$=\frac{C_\delta}{(\ln N)^{1+\delta}}\left\{1+\frac{(1+\delta)^2}{2}\frac{\ln\ln N}{\ln N}+O\left(\frac{1}{\ln N}\right)\right\},$$

$$D_o(Q_N^U)=\frac{2C_\delta}{\delta}\frac{1}{\ln(2+x_K)^\delta}(1+o_N(1))$$

$$=\frac{2C_\delta}{\delta(\ln N)^\delta}\left\{1+\frac{\delta(1+\delta)}{2}\frac{\ln\ln N}{\ln N}+O\left(\frac{1}{\ln N}\right)\right\}.$$

The ratio $\frac{D_o(Q_N^U)}{D_i(Q_N^U)}=\frac{\delta}{2}\ln N(1+o_N(1))$ indicates that D_o is dominant but that its dominance is logarithmic.

4.3.2 Optimal Nonuniform Quantizers

For a nonuniform quantizer Q_N^* optimized for the H-N density with parameter $\delta>2$, we use the differentiation method[8] to find the following outermost threshold:

$$\ln(2+x_K)=\left(\frac{\delta-2}{3}\right)^{\frac{3}{\delta+1}}(\ln 2)^{\frac{\delta-2}{\delta+1}}N^{\frac{3}{\delta+1}}$$

$$\times\left\{1+\left(\frac{3}{1+\delta}\right)\left(\frac{3\ln 2}{\delta-2}\right)^{\frac{\delta-2}{\delta+1}}\frac{1}{N^{(\delta-2)/(\delta+1)}}(1+o_N(1))\right\}.$$

The formula states that x_K of Q_N^* is asymptotically in the form of $e^{cN^{3/(\delta+1)}}=e^{c2^{3R/(\delta+1)}}$ and grows exponential-exponentially with rate R.

For x_2 of Q_N^*, it can be shown that the first two terms of the Taylor series of $y_1=E[x|0\le X\le x_2]$ is given by $ax_2+bx_2^2$, where $a=\frac{1}{2}$ and $b=-\frac{\delta+1+\ln 2}{24\ln 2}$, and then from (13) that

$$x_2=\frac{12\ln 2}{\delta-2}\frac{1}{N}\left\{1+\frac{3\ln 2+5-\delta}{\delta-2}\frac{1}{N}+O\left(\frac{1}{N^2}\right)\right\}. \quad (21)$$

We obtain from (15) the optimal outermost level y_K straightforwardly

$$y_K=\frac{1}{2^\delta}\frac{\Gamma(-\delta,\ln(2+x_K))}{\Gamma(-\delta,2\ln(2+x_K))}-2$$

and from applying (16) its asymptotic expression

$$y_K=2(x_K+1)-(\delta+1)\frac{(x_K+2)}{\ln(2+x_K)},\ x_K\to\infty.$$

Then we obtain for $\delta>2$

$$D_i(Q_N^*)=\frac{18C_\delta}{(\delta-2)^3(\ln 2)^{\delta-2}}\frac{1}{N^2}$$

$$\times\left\{1+O\left(\frac{1}{N^{(\delta-2)/(\delta+1)}}\right)+o_N(1)\right\},$$

$$D_o(Q_N^*)=\frac{2C_\delta}{\delta\left(\frac{\delta-2}{3}\right)^{\frac{3\delta}{\delta+1}}(\ln 2)^{\frac{\delta(\delta-2)}{\delta+1}}}\frac{1}{N^{\frac{3\delta}{\delta+1}}}$$

$$\times\left\{1+O\left(\frac{1}{N^{\frac{\min(3,\delta-2)}{\delta+1}}}\right)\right\}.$$

It is interesting to note for the unit-variance H-N pdf ($\delta=2.3863$) that $D_o(Q_N^*)$ is in the order of $\frac{1}{N^{3\delta(\delta+1)}}=\frac{1}{N^{2.1141}}$ and the ratio $\frac{D_o(Q_N^*)}{D_i(Q_N^*)}$ is of $\frac{1}{N^{0.1141}}$, exhibiting that $D_i(Q_N^*)$ is dominant and that its dominance is stronger than logarithmic but much weaker than linear in N. This contrasts to the situation of uniform quantizers, in which case $D_o(Q_N^U)$ is logarithmically dominant over $D_i(Q_N^U)$.

4.3.3 Numerical Results and Discussion

The left subfigure of Fig. 11 compares the thresholds x_2 and x_K with their corresponding asymptotic formulas listed in Table 2. It is observed that x_2^U and x_K^U start at 0.9739 at $R=2$ and, respectively, decreases to 0.0941 and increases to 49,299 at $R=20$ and, as R increases, they become bounded from below by the one- and from above by the two-term asymptotic formulas, both of which are approximately 20% below and 30 to 40% above the true values for $R=13$ to 20, respectively. The right subfigure is for x_2^* and x_K^*, which start at 1.6597 at $R=2$ and, respectively, decreases to 0.0055 and increases to 1.507×10^{114} at $R=11$, above which the design of quantizers has been numerically challenging.

Fig. 12 compares the distortions and asymptotic

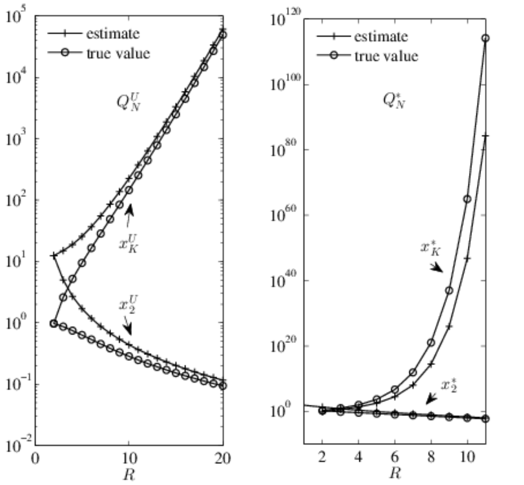

Fig. 11. Optimal thresholds x_x^U, x_2^*, x_K^U, x_K^* for the unit-variance H-N pdf

Table 2. Asymptotic formulas for optimal quantizers for the unit-variance H-N pdf

Q_N^U	x_2^U	$\frac{6.4479}{(\ln N)^{1.6932}}\left(1+2.8669\frac{\ln\ln N}{\ln N}\right)$
	x_K^U	$\frac{3.2239N}{(\ln N)^{1.6932}}\left(1+2.8669\frac{\ln\ln N}{\ln N}\right)$
	$D_i(Q_N^U)$	$\frac{3.4646}{(\ln N)^{3.3864}}$
	$D_o(Q_N^U)$	$\frac{2.9036}{(\ln N)^{2.3864}}\left(1+4.0405\frac{\ln\ln N}{\ln N}\right)$
	$D(Q_N^U)$	$\frac{C_{HN}}{(\ln N)^{2.3864}}\left(1+4.0405\frac{\ln\ln N}{\ln N}\right)$
		$C_{HN}=2.9036$
Q_N^*	x_2^*	$\frac{21.5284}{N}\left(1+\frac{12.1468}{N}\right)$
	$\ln(2+x_K^*)$	$0.1561N^{0.8859}\left(1+\frac{1.0735}{N^{0.1141}}\right)$
	$D_i(Q_N^*)$	$\frac{1245.7609}{N^2}$
	$D_o(Q_N^*)$	$\frac{244.3943}{N^{2.1141}}$
	$D(Q_N^*)$	$\frac{C_{PD}}{N^2}$; $C_{PD}=1245.7609$

formulas. It is observed that $(\ln N)^{\delta}D(Q_N^U)$ becomes to exceed $C_{HN}=2.9036$, is upperbounded by the two-term formula $C_{HN}\left(1+4.0405\frac{\ln\ln N}{\ln N}\right)$. The C_{HN} stay approximately at 65% of the true values for $R\geq 10$, while the two-term formula steadily decreases from 40% above the true value at $R=10$

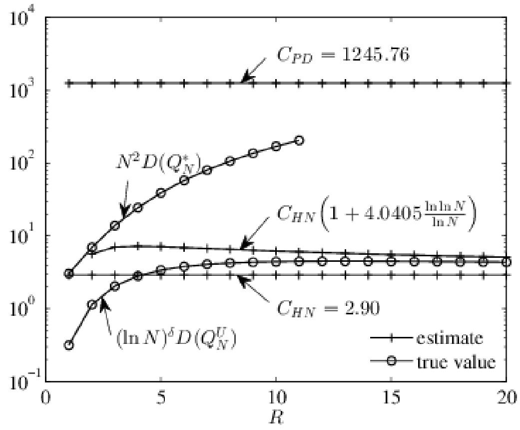

Fig. 12. Distortions $D(Q_N^U)$ and $D(Q_N^*)$ and their asymptotes for the unit-variance H-N pdf

to 22% at $R=20$. The behavior of $N^2D(Q_N^*)$ is also shown against $C_{PD}=1245.7609$ with its value reaching 204.9914 at $R=11$. As noted in Section II, Bucklew and Wise's finite moment condition is not satisfied in the case of any H-N pdf, so the convergence of $N^2D(Q_N^*)$ to C_{PD} has not yet been established rigorously.

We conclude from the observation that for $R\geq 5$,

$$\frac{C_{HN}}{(\ln N)^{\delta}}\leq D(Q_N^U)\leq\frac{C_{HN}}{(\ln N)^{\delta}}\left\{1+\frac{\delta(\delta+1)}{2}\frac{\ln\ln N}{\ln N}\right\}$$

and that for the studied bit range

$$D(Q_N^*)\ll\frac{C_{PD}}{N^2}.$$

V. Concluding Remarks

Some key characteristics of optimal symmetric uniform and nonuniform quantizers for the generalized gamma, Bucklew-Gallagher, and Hui-Neuhoff density functions have been compared with their asymptotic formulas either available from the previous studies or newly derived in this paper. They include the inner- and outermost thresholds, and the inner, outer and total MSE distortions. It is a pleasant surprise to observe that the formulas for the Bucklew-Gallagher density are generally accurate, as in the case of the common generalized gamma densities (when more tolerance being allowed for uniform quantizers for the usual gamma density). On the other hand, the formulas for the Hui-Neuhoff density do not enjoy the same accuracy at the studied rates but still seem suggestive of convergence, providing at the studied rates fairly reasonable bounds in the case of uniform quantizers and a still grossly loose bound in the nonuniform. This poor accuracy is attributed to a very heavy tail of the density, whose other manifestations include a challenge in numerical design of quantizers at high rates, and dominance reversal of the inner distortion in that it, while dominated by the outer distortion in the uniform quantizers, gains dominance in the nonuniform. A similar dominance shift occurs in a lesser degree to the Bucklew-Gallagher density, for which the inner distortion, equally important with the outer distortion in the uniform quantizers, becomes dominant in the nonuniform.

Also investigated is the uniqueness problem associated with the differentiation method for finding optimal step sizes of uniform quantizers. The method has been observed to yield unique solutions for the common generalized gamma, Bucklew-Gallagher, and Hui-Neuhoff densities, because the distortion function in such cases has a unique local minimum and furthermore, in many cases, is convex-U in the step size. In addition there have been found many generalized gamma densities whose distortion functions exhibit multiple local minimizers, the smallest among which, nevertheless, always seems to be globally optimal.

References

[1] S. Yoo and S. Y. Kim, "Conversion loss for the quantizer of GPS civil receiver in heavy wideband gaussian noise environments," *J. KICS*, vol. 38A, no. 9, pp. 792-797, Sept. 2013.

[2] D. Lee and W. Sung, "Adaptive quantization scheme for multi-level cell NAND flash memory," *J. KICS*, vol. 38C, no. 6, pp. 540-549, Jun. 2013.

[3] B. Hong and W. Choi, "Distributed MIMO systems based on quantize-map-and-forward (QMF) relaying," *J. KICS*, vol. 39A, no. 7, pp. 404-412, Jul. 2014.

[4] P. F. Panter and W. Dite, "Quantization distortion in pulse-count modulation with nonuniform spacing of levels," in *Proc. IRE*, vol. 39, pp. 44-48, 1951.

[5] J. A. Bucklew and N. C. Gallagher, "Some properties of uniform step size quantizers," *IEEE Trans. Inf. Theory*, vol. 26, pp. 610-613, 1980.

[6] J. A. Bucklew and G. L. Wise, "Multi-dimensional asymptotic quantization theory with r th power distortion measures," *IEEE Trans. Inf. Theory*, vol. 28, pp. 239-247, 1982.

[7] D. Hui and D. L. Neuhoff, "Asymptotic analysis of optimal fixed-rate uniform scalar quantization," *IEEE Trans. Inf. Theory*, vol. 47, pp. 957-977, 2001.

[8] S. Na and D. L. Neuhoff, "On the support of MSE-optimal, fixed-rate, scalar quantizers," *IEEE Trans. Inf. Theory*, vol. 47, pp. 2972-2982, 2001.

[9] S. Na and D. L. Neuhoff, "Asymptotic MSE distortion of mismatched uniform scalar quantization," *IEEE Trans. Inf. Theory*, vol. 58, pp. 3169-3181, 2012.

[10] J. Rhee and S. Na, "Asymptotic characteristics of MSE-optimal scalar quantizers for generalized gamma sources," *J. KICS*, vol. 37, no. 5, pp. 279-289, May 2012.

[11] S. P. Lloyd, "Least squares quantization in PCM," *IEEE Trans. Inf. Theory*, vol. 28, pp. 129-137, 1982.

[12] J. Max, "Quantizing for minimum distortion," *IRE Trans. Inf. Theory*, vol. 46, pp. 7-12, 1960.

[13] E. W. Stacy, "A generalization of the gamma distribution," *Ann. Math. Stat.*, vol. 33, no. 3, pp. 1187-1192, Sept. 1962.

[14] F. W. J. Olver, *Asymptotics and Special Functions*, 2nd Ed., A K Peters/CRC Press, 1997.

이 재 건 (Jagan Rhee)
1992년 : 아주대 전자공학 학사
1994년 : 아주대 전자공학 석사
2012년 : 아주대 전자공학 박사

나 상 신 (Sangsin Na)
1982년 : 서울대 전자공학 학사
1989년 : 미시간대 전기및전자계산학 박사
1989년~1991년 : 네브라스카대 전기공학과 조교수
1991년~현재 : 아주대 전자공학과 교수

Appendix

Table 3. Unit-variance Gaussian pdf $p(x) = \frac{1}{\sqrt{2\pi}} e^{-\frac{x^2}{2}}$

	R	x_2	y_1	x_K	y_K	D_t	D_i	D_o
	1		7.979×10^{-1}	0.000×10^{0}	7.979×10^{-1}	3.634×10^{-1}	0.000×10^{0}	3.634×10^{-1}
	2	9.957×10^{-1}	4.978×10^{-1}	9.957×10^{-1}	1.494×10^{0}	1.188×10^{-1}	5.484×10^{-2}	6.401×10^{-2}
	3	5.860×10^{-1}	2.930×10^{-1}	1.758×10^{0}	2.051×10^{0}	3.744×10^{-2}	2.627×10^{-2}	1.117×10^{-2}
	4	3.352×10^{-1}	1.676×10^{-1}	2.346×10^{0}	2.514×10^{0}	1.154×10^{-2}	9.182×10^{-3}	2.361×10^{-3}
	5	1.881×10^{-1}	9.407×10^{-2}	2.822×10^{0}	2.916×10^{0}	3.495×10^{-3}	2.935×10^{-3}	5.597×10^{-4}
	6	1.041×10^{-1}	5.203×10^{-2}	3.226×10^{0}	3.278×10^{0}	1.040×10^{-3}	9.013×10^{-4}	1.388×10^{-4}
	7	5.687×10^{-2}	2.843×10^{-2}	3.583×10^{0}	3.611×10^{0}	3.043×10^{-4}	2.694×10^{-4}	3.493×10^{-5}
	8	3.076×10^{-2}	1.538×10^{-2}	3.907×10^{0}	3.922×10^{0}	8.769×10^{-5}	7.885×10^{-5}	8.833×10^{-6}
Q_N^U	9	1.650×10^{-2}	8.249×10^{-3}	4.207×10^{0}	4.215×10^{0}	2.492×10^{-5}	2.268×10^{-5}	2.235×10^{-6}
	10	8.785×10^{-3}	4.393×10^{-3}	4.489×10^{0}	4.494×10^{0}	6.997×10^{-6}	6.432×10^{-6}	5.650×10^{-7}
	11	4.650×10^{-3}	2.325×10^{-3}	4.757×10^{0}	4.759×10^{0}	1.944×10^{-6}	1.802×10^{-6}	1.427×10^{-7}
	12	2.448×10^{-3}	1.224×10^{-3}	5.012×10^{0}	5.013×10^{0}	5.355×10^{-7}	4.996×10^{-7}	3.598×10^{-8}
	13	1.284×10^{-3}	6.418×10^{-4}	5.256×10^{0}	5.257×10^{0}	1.464×10^{-7}	1.373×10^{-7}	9.062×10^{-9}
	14	6.705×10^{-4}	3.352×10^{-4}	5.492×10^{0}	5.492×10^{0}	3.974×10^{-8}	3.746×10^{-8}	2.281×10^{-9}
	15	3.491×10^{-4}	1.745×10^{-4}	5.719×10^{0}	5.719×10^{0}	1.073×10^{-8}	1.015×10^{-8}	5.734×10^{-10}
	16	1.812×10^{-4}	9.061×10^{-5}	5.938×10^{0}	5.938×10^{0}	2.881×10^{-9}	2.737×10^{-9}	1.441×10^{-10}
	17	9.386×10^{-5}	4.693×10^{-5}	6.151×10^{0}	6.151×10^{0}	7.703×10^{-10}	7.341×10^{-10}	3.618×10^{-11}
	18	4.850×10^{-5}	2.425×10^{-5}	6.357×10^{0}	6.357×10^{0}	2.051×10^{-10}	1.960×10^{-10}	9.085×10^{-12}
	19	2.502×10^{-5}	1.251×10^{-5}	6.558×10^{0}	6.558×10^{0}	5.444×10^{-11}	5.216×10^{-11}	2.278×10^{-12}
	20	1.288×10^{-5}	6.441×10^{-6}	6.754×10^{0}	6.754×10^{0}	1.440×10^{-11}	1.383×10^{-11}	5.721×10^{-13}
	1		7.979×10^{-1}	0.000×10^{0}	7.979×10^{-1}	3.634×10^{-1}	0.000×10^{0}	3.634×10^{-1}
	2	9.816×10^{-1}	4.528×10^{-1}	9.816×10^{-1}	1.510×10^{0}	1.175×10^{-1}	5.181×10^{-2}	6.567×10^{-2}
	3	5.005×10^{-1}	2.451×10^{-1}	1.748×10^{0}	2.152×10^{0}	3.455×10^{-2}	2.404×10^{-2}	1.051×10^{-2}
	4	2.582×10^{-1}	1.284×10^{-1}	2.401×10^{0}	2.733×10^{0}	9.501×10^{-3}	7.974×10^{-3}	1.527×10^{-3}
	5	1.320×10^{-1}	6.589×10^{-2}	2.976×10^{0}	3.261×10^{0}	2.505×10^{-3}	2.296×10^{-3}	2.083×10^{-4}
	6	6.684×10^{-2}	3.341×10^{-2}	3.492×10^{0}	3.744×10^{0}	6.442×10^{-4}	6.169×10^{-4}	2.735×10^{-5}
	7	3.366×10^{-2}	1.683×10^{-2}	3.962×10^{0}	4.190×10^{0}	1.635×10^{-4}	1.600×10^{-4}	3.515×10^{-6}
Q_N^*	8	1.689×10^{-2}	8.446×10^{-3}	4.395×10^{0}	4.604×10^{0}	4.119×10^{-5}	4.074×10^{-5}	4.463×10^{-7}
	9	8.463×10^{-3}	4.231×10^{-3}	4.797×10^{0}	4.991×10^{0}	1.034×10^{-5}	1.028×10^{-5}	5.630×10^{-8}
	10	4.236×10^{-3}	2.118×10^{-3}	5.174×10^{0}	5.355×10^{0}	2.589×10^{-6}	2.582×10^{-6}	7.078×10^{-9}
	11	2.119×10^{-3}	1.059×10^{-3}	5.529×10^{0}	5.700×10^{0}	6.480×10^{-7}	6.471×10^{-7}	8.883×10^{-10}
	12	1.060×10^{-3}	5.298×10^{-4}	5.866×10^{0}	6.028×10^{0}	1.621×10^{-7}	1.620×10^{-7}	1.111×10^{-10}
	13	5.299×10^{-4}	2.650×10^{-4}	6.186×10^{0}	6.340×10^{0}	4.053×10^{-8}	4.052×10^{-8}	1.401×10^{-11}
	14	2.650×10^{-4}	1.325×10^{-4}	6.496×10^{0}	6.644×10^{0}	1.013×10^{-8}	1.013×10^{-8}	1.721×10^{-12}
	15	1.325×10^{-4}	6.625×10^{-5}	6.799×10^{0}	6.943×10^{0}	2.534×10^{-9}	2.533×10^{-9}	2.034×10^{-13}
	16	6.630×10^{-5}	3.315×10^{-5}	7.093×10^{0}	7.236×10^{0}	6.334×10^{-10}	6.334×10^{-10}	2.345×10^{-14}

Table 4. Unit-variance two-sided Rayleigh pdf $p(x) = |x| e^{-x^2}$

	R	x_2	y_1	x_K	y_K	D_t	D_i	D_o
	1		8.862×10^{-1}	0.000×10^{0}	8.862×10^{-1}	2.146×10^{-1}	0.000×10^{0}	2.146×10^{-1}
	2	8.946×10^{-1}	4.473×10^{-1}	8.946×10^{-1}	1.342×10^{0}	8.091×10^{-2}	3.137×10^{-2}	4.954×10^{-2}
	3	4.955×10^{-1}	2.478×10^{-1}	1.487×10^{0}	1.734×10^{0}	2.499×10^{-2}	1.774×10^{-2}	7.243×10^{-3}
	4	2.747×10^{-1}	1.374×10^{-1}	1.923×10^{0}	2.061×10^{0}	7.464×10^{-3}	6.097×10^{-3}	1.367×10^{-3}
	5	1.510×10^{-1}	7.552×10^{-2}	2.266×10^{0}	2.341×10^{0}	2.197×10^{-3}	1.887×10^{-3}	3.098×10^{-4}
	6	8.228×10^{-2}	4.114×10^{-2}	2.551×10^{0}	2.592×10^{0}	6.382×10^{-4}	5.630×10^{-4}	7.520×10^{-5}
	7	4.444×10^{-2}	2.222×10^{-2}	2.799×10^{0}	2.822×10^{0}	1.832×10^{-4}	1.645×10^{-4}	1.869×10^{-5}
	8	2.381×10^{-2}	1.191×10^{-2}	3.024×10^{0}	3.036×10^{0}	5.193×10^{-5}	4.725×10^{-5}	4.684×10^{-6}
Q_N^U	9	1.267×10^{-2}	6.337×10^{-3}	3.232×10^{0}	3.238×10^{0}	1.456×10^{-5}	1.338×10^{-5}	1.177×10^{-6}
	10	6.705×10^{-3}	3.353×10^{-3}	3.426×10^{0}	3.430×10^{0}	4.042×10^{-6}	3.747×10^{-6}	2.959×10^{-7}
	11	3.529×10^{-3}	1.765×10^{-3}	3.611×10^{0}	3.612×10^{0}	1.112×10^{-6}	1.038×10^{-6}	7.438×10^{-8}
	12	1.850×10^{-3}	9.249×10^{-4}	3.787×10^{0}	3.787×10^{0}	3.038×10^{-7}	2.851×10^{-7}	1.869×10^{-8}
	13	9.658×10^{-4}	4.829×10^{-4}	3.955×10^{0}	3.956×10^{0}	8.243×10^{-8}	7.774×10^{-8}	4.692×10^{-9}
	14	5.027×10^{-4}	2.513×10^{-4}	4.117×10^{0}	4.118×10^{0}	2.223×10^{-8}	2.106×10^{-8}	1.178×10^{-9}
	15	2.609×10^{-4}	1.304×10^{-4}	4.274×10^{0}	4.274×10^{0}	5.967×10^{-9}	5.672×10^{-9}	2.954×10^{-10}
	16	1.351×10^{-4}	6.753×10^{-5}	4.426×10^{0}	4.426×10^{0}	1.594×10^{-9}	1.520×10^{-9}	7.409×10^{-11}
	17	6.977×10^{-5}	3.489×10^{-5}	4.573×10^{0}	4.573×10^{0}	4.243×10^{-10}	4.057×10^{-10}	1.857×10^{-11}
	18	3.598×10^{-5}	1.799×10^{-5}	4.715×10^{0}	4.715×10^{0}	1.125×10^{-10}	1.079×10^{-10}	4.655×10^{-12}
	19	1.852×10^{-5}	9.259×10^{-6}	4.854×10^{0}	4.854×10^{0}	2.974×10^{-11}	2.858×10^{-11}	1.167×10^{-12}
	20	9.517×10^{-6}	4.758×10^{-6}	4.990×10^{0}	4.990×10^{0}	7.840×10^{-12}	7.548×10^{-12}	2.925×10^{-13}
	1		8.862×10^{-1}	0.000×10^{0}	8.862×10^{-1}	2.146×10^{-1}	0.000×10^{0}	2.146×10^{-1}
	2	9.721×10^{-1}	5.863×10^{-1}	9.721×10^{-1}	1.358×10^{0}	7.315×10^{-2}	3.386×10^{-2}	3.929×10^{-2}
	3	5.811×10^{-1}	3.743×10^{-1}	1.504×10^{0}	1.788×10^{0}	2.236×10^{-2}	1.574×10^{-2}	6.623×10^{-3}
	4	3.530×10^{-1}	2.324×10^{-1}	1.951×10^{0}	2.182×10^{0}	6.306×10^{-3}	5.308×10^{-3}	9.982×10^{-4}
	5	2.134×10^{-1}	1.416×10^{-1}	2.346×10^{0}	2.544×10^{0}	1.687×10^{-3}	1.547×10^{-3}	1.391×10^{-4}
	6	1.282×10^{-1}	8.533×10^{-2}	2.702×10^{0}	2.876×10^{0}	4.373×10^{-4}	4.188×10^{-4}	1.849×10^{-5}
	7	7.669×10^{-2}	5.110×10^{-2}	3.026×10^{0}	3.184×10^{0}	1.114×10^{-4}	1.090×10^{-4}	2.391×10^{-6}
Q_N^*	8	4.575×10^{-2}	3.049×10^{-2}	3.325×10^{0}	3.470×10^{0}	2.813×10^{-5}	2.782×10^{-5}	3.046×10^{-7}
	9	2.725×10^{-2}	1.817×10^{-2}	3.604×10^{0}	3.738×10^{0}	7.068×10^{-6}	7.029×10^{-6}	3.848×10^{-8}
	10	1.622×10^{-2}	1.081×10^{-2}	3.865×10^{0}	3.990×10^{0}	1.771×10^{-6}	1.767×10^{-6}	4.842×10^{-9}
	11	9.648×10^{-3}	6.432×10^{-3}	4.111×10^{0}	4.229×10^{0}	4.434×10^{-7}	4.428×10^{-7}	6.077×10^{-10}
	12	5.738×10^{-3}	3.825×10^{-3}	4.345×10^{0}	4.457×10^{0}	1.109×10^{-7}	1.108×10^{-7}	7.620×10^{-11}
	13	3.412×10^{-3}	2.275×10^{-3}	4.568×10^{0}	4.675×10^{0}	2.774×10^{-8}	2.773×10^{-8}	9.536×10^{-12}
	14	2.029×10^{-3}	1.353×10^{-3}	4.781×10^{0}	4.884×10^{0}	6.936×10^{-9}	6.935×10^{-9}	1.193×10^{-12}
	15	1.206×10^{-3}	8.043×10^{-4}	4.987×10^{0}	5.085×10^{0}	1.734×10^{-9}	1.734×10^{-9}	1.482×10^{-13}
	16	7.174×10^{-4}	4.783×10^{-4}	5.184×10^{0}	5.280×10^{0}	4.336×10^{-10}	4.335×10^{-10}	1.844×10^{-14}

Table 5. Unit-variance Laplacian pdf $p(x)=\frac{1}{\sqrt{2}}e^{-\sqrt{2}|x|}$

	R	x_2	y_1	x_K	y_K	D_t	D_i	D_o
Q_N^U	1		7.071×10^{-1}	0.000×10^{0}	7.071×10^{-1}	5.000×10^{-1}	0.000×10^{0}	5.000×10^{-1}
	2	1.087×10^{0}	5.437×10^{-1}	1.087×10^{0}	1.631×10^{0}	1.963×10^{-1}	8.314×10^{-2}	1.132×10^{-1}
	3	7.309×10^{-1}	3.655×10^{-1}	2.193×10^{0}	2.558×10^{0}	7.175×10^{-2}	4.400×10^{-2}	2.775×10^{-2}
	4	4.610×10^{-1}	2.305×10^{-1}	3.227×10^{0}	3.457×10^{0}	2.535×10^{-2}	1.777×10^{-2}	7.580×10^{-3}
	5	2.800×10^{-1}	1.400×10^{-1}	4.200×10^{0}	4.340×10^{0}	8.713×10^{-3}	6.550×10^{-3}	2.164×10^{-3}
	6	1.657×10^{-1}	8.284×10^{-2}	5.136×10^{0}	5.219×10^{0}	2.913×10^{-3}	2.290×10^{-3}	6.233×10^{-4}
	7	9.610×10^{-2}	4.805×10^{-2}	6.054×10^{0}	6.102×10^{0}	9.486×10^{-4}	7.699×10^{-4}	1.787×10^{-4}
	8	5.484×10^{-2}	2.742×10^{-2}	6.965×10^{0}	6.993×10^{0}	3.014×10^{-4}	2.507×10^{-4}	5.072×10^{-5}
	9	3.088×10^{-2}	1.544×10^{-2}	7.875×10^{0}	7.891×10^{0}	9.373×10^{-5}	7.948×10^{-5}	1.425×10^{-5}
	10	1.720×10^{-2}	8.598×10^{-3}	8.787×10^{0}	8.796×10^{0}	2.860×10^{-5}	2.464×10^{-5}	3.962×10^{-6}
	11	9.484×10^{-3}	4.742×10^{-3}	9.702×10^{0}	9.707×10^{0}	8.587×10^{-6}	7.495×10^{-6}	1.092×10^{-6}
	12	5.189×10^{-3}	2.594×10^{-3}	1.062×10^{1}	1.062×10^{1}	2.542×10^{-6}	2.243×10^{-6}	2.986×10^{-7}
	13	2.819×10^{-3}	1.409×10^{-3}	1.154×10^{1}	1.155×10^{1}	7.433×10^{-7}	6.622×10^{-7}	8.112×10^{-8}
	14	1.522×10^{-3}	7.612×10^{-4}	1.247×10^{1}	1.247×10^{1}	2.151×10^{-7}	1.931×10^{-7}	2.190×10^{-8}
	15	8.179×10^{-4}	4.090×10^{-4}	1.340×10^{1}	1.340×10^{1}	6.163×10^{-8}	5.575×10^{-8}	5.884×10^{-9}
	16	4.374×10^{-4}	2.187×10^{-4}	1.433×10^{1}	1.433×10^{1}	1.752×10^{-8}	1.594×10^{-8}	1.573×10^{-9}
	17	2.330×10^{-4}	1.165×10^{-4}	1.527×10^{1}	1.527×10^{1}	4.942×10^{-9}	4.523×10^{-9}	4.190×10^{-10}
	18	1.236×10^{-4}	6.182×10^{-5}	1.621×10^{1}	1.621×10^{1}	1.385×10^{-9}	1.274×10^{-9}	1.112×10^{-10}
	19	6.541×10^{-5}	3.271×10^{-5}	1.715×10^{1}	1.715×10^{1}	3.860×10^{-10}	3.566×10^{-10}	2.940×10^{-11}
	20	3.450×10^{-5}	1.725×10^{-5}	1.809×10^{1}	1.809×10^{1}	1.070×10^{-10}	9.921×10^{-11}	7.754×10^{-12}
Q_N^*	1		7.071×10^{-1}	0.000×10^{0}	7.071×10^{-1}	5.000×10^{-1}	0.000×10^{0}	5.000×10^{-1}
	2	1.127×10^{0}	4.198×10^{-1}	1.127×10^{0}	1.834×10^{0}	1.762×10^{-1}	7.460×10^{-2}	1.016×10^{-1}
	3	5.332×10^{-1}	2.334×10^{-1}	2.380×10^{0}	3.087×10^{0}	5.448×10^{-2}	3.720×10^{-2}	1.728×10^{-2}
	4	2.644×10^{-1}	1.240×10^{-1}	3.724×10^{0}	4.431×10^{0}	1.537×10^{-2}	1.279×10^{-2}	2.581×10^{-3}
	5	1.322×10^{-1}	6.405×10^{-2}	5.126×10^{0}	5.833×10^{0}	4.102×10^{-3}	3.747×10^{-3}	3.554×10^{-4}
	6	6.618×10^{-2}	3.257×10^{-2}	6.560×10^{0}	7.268×10^{0}	1.061×10^{-3}	1.014×10^{-3}	4.673×10^{-5}
	7	3.311×10^{-2}	1.643×10^{-2}	8.013×10^{0}	8.720×10^{0}	2.699×10^{-4}	2.639×10^{-4}	5.995×10^{-6}
	8	1.656×10^{-2}	8.250×10^{-3}	9.474×10^{0}	1.018×10^{1}	6.806×10^{-5}	6.730×10^{-5}	7.593×10^{-7}
	9	8.284×10^{-3}	4.134×10^{-3}	1.094×10^{1}	1.165×10^{1}	1.709×10^{-5}	1.699×10^{-5}	9.554×10^{-8}
	10	4.143×10^{-3}	2.069×10^{-3}	1.241×10^{1}	1.311×10^{1}	4.282×10^{-6}	4.270×10^{-6}	1.198×10^{-8}
	11	2.071×10^{-3}	1.035×10^{-3}	1.388×10^{1}	1.458×10^{1}	1.072×10^{-6}	1.070×10^{-6}	1.500×10^{-9}
	12	1.036×10^{-3}	5.178×10^{-4}	1.535×10^{1}	1.605×10^{1}	2.681×10^{-7}	2.679×10^{-7}	1.875×10^{-10}
	13	5.179×10^{-4}	2.589×10^{-4}	1.682×10^{1}	1.753×10^{1}	6.704×10^{-8}	6.701×10^{-8}	2.334×10^{-11}
	14	2.589×10^{-4}	1.295×10^{-4}	1.830×10^{1}	1.901×10^{1}	1.676×10^{-8}	1.676×10^{-8}	2.890×10^{-12}
	15	1.295×10^{-4}	6.474×10^{-5}	1.970×10^{1}	2.039×10^{1}	4.191×10^{-9}	4.190×10^{-9}	3.962×10^{-13}
	16	6.476×10^{-5}	3.238×10^{-5}	2.136×10^{1}	2.211×10^{1}	1.048×10^{-9}	1.048×10^{-9}	3.817×10^{-14}

Table 6. Unit-variance gamma pdf $p(x)=\frac{3^{1/4}}{2\sqrt{2\pi|x|}}e^{-\frac{\sqrt{3}|x|}{2}}$

	R	x_2	y_1	x_K	y_K	D_t	D_i	D_o
Q_N^U	1		5.774×10^{-1}	0.000×10^{0}	5.774×10^{-1}	6.667×10^{-1}	0.000×10^{0}	6.667×10^{-1}
	2	1.066×10^{0}	5.330×10^{-1}	1.066×10^{0}	1.599×10^{0}	3.200×10^{-1}	1.215×10^{-1}	1.985×10^{-1}
	3	7.957×10^{-1}	3.979×10^{-1}	2.387×10^{0}	2.785×10^{0}	1.323×10^{-1}	7.150×10^{-2}	6.083×10^{-2}
	4	5.400×10^{-1}	2.700×10^{-1}	3.780×10^{0}	4.050×10^{0}	5.008×10^{-2}	3.191×10^{-2}	1.817×10^{-2}
	5	3.459×10^{-1}	1.730×10^{-1}	5.189×10^{0}	5.362×10^{0}	1.784×10^{-2}	1.251×10^{-2}	5.331×10^{-3}
	6	2.130×10^{-1}	1.065×10^{-1}	6.603×10^{0}	6.710×10^{0}	6.073×10^{-3}	4.534×10^{-3}	1.538×10^{-3}
	7	1.273×10^{-1}	6.366×10^{-2}	8.021×10^{0}	8.084×10^{0}	1.996×10^{-3}	1.558×10^{-3}	4.377×10^{-4}
	8	7.436×10^{-2}	3.718×10^{-2}	9.444×10^{0}	9.481×10^{0}	6.379×10^{-4}	5.148×10^{-4}	1.231×10^{-4}
	9	4.264×10^{-2}	2.132×10^{-2}	1.087×10^{1}	1.090×10^{1}	1.993×10^{-4}	1.650×10^{-4}	3.427×10^{-5}
	10	2.410×10^{-2}	1.205×10^{-2}	1.231×10^{1}	1.233×10^{1}	6.107×10^{-5}	5.161×10^{-5}	9.467×10^{-6}
	11	1.345×10^{-2}	6.725×10^{-3}	1.376×10^{1}	1.377×10^{1}	1.842×10^{-5}	1.583×10^{-5}	2.598×10^{-6}
	12	7.433×10^{-3}	3.717×10^{-3}	1.522×10^{1}	1.522×10^{1}	5.483×10^{-6}	4.774×10^{-6}	7.087×10^{-7}
	13	4.073×10^{-3}	2.037×10^{-3}	1.668×10^{1}	1.668×10^{1}	1.613×10^{-6}	1.420×10^{-6}	1.923×10^{-7}
	14	2.216×10^{-3}	1.108×10^{-3}	1.815×10^{1}	1.815×10^{1}	4.694×10^{-7}	4.174×10^{-7}	5.197×10^{-8}
	15	1.198×10^{-3}	5.990×10^{-4}	1.963×10^{1}	1.963×10^{1}	1.354×10^{-7}	1.214×10^{-7}	1.398×10^{-8}
	16	6.443×10^{-4}	3.222×10^{-4}	2.111×10^{1}	2.111×10^{1}	3.872×10^{-8}	3.497×10^{-8}	3.747×10^{-9}
	17	3.449×10^{-4}	1.724×10^{-4}	2.260×10^{1}	2.260×10^{1}	1.099×10^{-8}	9.992×10^{-9}	1.001×10^{-9}
	18	1.839×10^{-4}	9.193×10^{-5}	2.410×10^{1}	2.410×10^{1}	3.100×10^{-9}	2.833×10^{-9}	2.663×10^{-10}
	19	9.766×10^{-5}	4.883×10^{-5}	2.560×10^{1}	2.560×10^{1}	8.688×10^{-10}	7.981×10^{-10}	7.065×10^{-11}
	20	5.170×10^{-5}	2.585×10^{-5}	2.711×10^{1}	2.711×10^{1}	2.421×10^{-10}	2.234×10^{-10}	1.870×10^{-11}
Q_N^*	1		5.774×10^{-1}	0.000×10^{0}	5.774×10^{-1}	6.667×10^{-1}	0.000×10^{0}	6.667×10^{-1}
	2	1.268×10^{0}	3.132×10^{-1}	1.268×10^{0}	2.223×10^{0}	2.318×10^{-1}	9.416×10^{-2}	1.377×10^{-1}
	3	5.274×10^{-1}	1.554×10^{-1}	3.089×10^{0}	4.121×10^{0}	7.047×10^{-2}	4.762×10^{-2}	2.285×10^{-2}
	4	2.299×10^{-1}	7.264×10^{-2}	5.128×10^{0}	6.195×10^{0}	1.961×10^{-2}	1.627×10^{-2}	3.341×10^{-3}
	5	1.008×10^{-1}	3.281×10^{-2}	7.293×10^{0}	8.380×10^{0}	5.185×10^{-3}	4.731×10^{-3}	4.533×10^{-4}
	6	4.411×10^{-2}	1.455×10^{-2}	9.530×10^{0}	1.063×10^{1}	1.334×10^{-3}	1.275×10^{-3}	5.908×10^{-5}
	7	1.927×10^{-2}	6.394×10^{-3}	1.181×10^{1}	1.292×10^{1}	3.382×10^{-4}	3.307×10^{-4}	7.541×10^{-6}
	8	8.404×10^{-3}	2.796×10^{-3}	1.412×10^{1}	1.523×10^{1}	8.517×10^{-5}	8.422×10^{-5}	9.524×10^{-7}
	9	3.663×10^{-3}	1.220×10^{-3}	1.644×10^{1}	1.756×10^{1}	2.137×10^{-5}	2.125×10^{-5}	1.197×10^{-7}
	10	1.595×10^{-3}	5.316×10^{-4}	1.877×10^{1}	1.990×10^{1}	5.352×10^{-6}	5.337×10^{-6}	1.499×10^{-8}
	11	6.946×10^{-4}	2.315×10^{-4}	2.111×10^{1}	2.224×10^{1}	1.339×10^{-6}	1.337×10^{-6}	1.878×10^{-9}
	12	3.024×10^{-4}	1.008×10^{-4}	2.346×10^{1}	2.459×10^{1}	3.349×10^{-7}	3.347×10^{-7}	2.338×10^{-10}
	13	1.316×10^{-4}	4.388×10^{-5}	2.584×10^{1}	2.699×10^{1}	8.375×10^{-8}	8.373×10^{-8}	2.851×10^{-11}
	14	5.731×10^{-5}	1.910×10^{-5}	2.808×10^{1}	2.918×10^{1}	2.094×10^{-8}	2.094×10^{-8}	3.970×10^{-12}
	15	2.495×10^{-5}	8.315×10^{-6}	3.095×10^{1}	3.223×10^{1}	5.236×10^{-9}	5.235×10^{-9}	3.216×10^{-13}
	16	1.086×10^{-5}	3.619×10^{-6}	3.278×10^{1}	3.392×10^{1}	1.309×10^{-9}	1.309×10^{-9}	6.285×10^{-14}

Table 7. Unit-variance Bucklew-Gallagher pdf $p(x)=\dfrac{3}{2(|x|+1)^4}$

	R	x_2	y_1	x_K	y_K	D_t	D_i	D_o
Q_N^U	1		5.000×10^{-1}	0.000×10^{0}	5.000×10^{-1}	7.500×10^{-1}	0.000×10^{0}	7.500×10^{-1}
	2	1.000×10^{0}	5.000×10^{-1}	1.000×10^{0}	1.500×10^{0}	5.000×10^{-1}	9.375×10^{-2}	4.063×10^{-1}
	3	8.918×10^{-1}	4.459×10^{-1}	2.675×10^{0}	3.121×10^{0}	3.226×10^{-1}	7.956×10^{-2}	2.431×10^{-1}
	4	7.618×10^{-1}	3.809×10^{-1}	5.332×10^{0}	5.713×10^{0}	2.056×10^{-1}	5.657×10^{-2}	1.490×10^{-1}
	5	6.364×10^{-1}	3.182×10^{-1}	9.546×10^{0}	9.864×10^{0}	1.302×10^{-1}	3.812×10^{-2}	9.205×10^{-2}
	6	5.243×10^{-1}	2.621×10^{-1}	1.625×10^{1}	1.651×10^{1}	8.214×10^{-2}	2.505×10^{-2}	5.709×10^{-2}
	7	4.276×10^{-1}	2.138×10^{-1}	2.694×10^{1}	2.715×10^{1}	5.175×10^{-2}	1.623×10^{-2}	3.552×10^{-2}
	8	3.461×10^{-1}	1.730×10^{-1}	4.395×10^{1}	4.412×10^{1}	3.258×10^{-2}	1.042×10^{-2}	2.216×10^{-2}
	9	2.785×10^{-1}	1.392×10^{-1}	7.101×10^{1}	7.115×10^{1}	2.051×10^{-2}	6.653×10^{-3}	1.386×10^{-2}
	10	2.231×10^{-1}	1.116×10^{-1}	1.140×10^{2}	1.141×10^{2}	1.291×10^{-2}	4.228×10^{-3}	8.686×10^{-3}
	11	1.782×10^{-1}	8.910×10^{-2}	1.823×10^{2}	1.824×10^{2}	8.132×10^{-3}	2.679×10^{-3}	5.453×10^{-3}
	12	1.420×10^{-1}	7.101×10^{-2}	2.907×10^{2}	2.908×10^{2}	5.121×10^{-3}	1.694×10^{-3}	3.427×10^{-3}
	13	1.130×10^{-1}	5.652×10^{-2}	4.629×10^{2}	4.629×10^{2}	3.226×10^{-3}	1.070×10^{-3}	2.156×10^{-3}
	14	8.987×10^{-2}	4.493×10^{-2}	7.361×10^{2}	7.362×10^{2}	2.032×10^{-3}	6.752×10^{-4}	1.357×10^{-3}
	15	7.141×10^{-2}	3.570×10^{-2}	1.170×10^{3}	1.170×10^{3}	1.280×10^{-3}	4.258×10^{-4}	8.540×10^{-4}
	16	5.672×10^{-2}	2.836×10^{-2}	1.858×10^{3}	1.858×10^{3}	8.062×10^{-4}	2.684×10^{-4}	5.378×10^{-4}
	17	4.504×10^{-2}	2.252×10^{-2}	2.951×10^{3}	2.951×10^{3}	5.079×10^{-4}	1.692×10^{-4}	3.387×10^{-4}
	18	3.576×10^{-2}	1.788×10^{-2}	4.686×10^{3}	4.686×10^{3}	3.199×10^{-4}	1.066×10^{-4}	2.133×10^{-4}
	19	2.838×10^{-2}	1.419×10^{-2}	7.441×10^{3}	7.441×10^{3}	2.015×10^{-4}	6.716×10^{-5}	1.344×10^{-4}
	20	2.253×10^{-2}	1.127×10^{-2}	1.181×10^{4}	1.181×10^{4}	1.270×10^{-4}	4.231×10^{-5}	8.465×10^{-5}
Q_N^*	1		5.000×10^{-1}	0.000×10^{0}	5.000×10^{-1}	7.500×10^{-1}	0.000×10^{0}	7.500×10^{-1}
	2	1.732×10^{0}	3.660×10^{-1}	1.732×10^{0}	3.098×10^{0}	4.019×10^{-1}	1.274×10^{-1}	2.745×10^{-1}
	3	7.531×10^{-1}	2.426×10^{-1}	8.755×10^{0}	1.363×10^{1}	1.765×10^{-1}	9.962×10^{-2}	7.688×10^{-2}
	4	3.686×10^{-1}	1.464×10^{-1}	4.420×10^{1}	6.680×10^{1}	6.426×10^{-2}	4.766×10^{-2}	1.659×10^{-2}
	5	1.848×10^{-1}	8.200×10^{-2}	2.577×10^{2}	3.870×10^{2}	2.017×10^{-2}	1.727×10^{-2}	2.899×10^{-3}
	6	9.291×10^{-2}	4.371×10^{-2}	1.711×10^{3}	2.567×10^{3}	5.731×10^{-3}	5.293×10^{-3}	4.382×10^{-4}
	7	4.664×10^{-2}	2.261×10^{-2}	1.237×10^{4}	1.855×10^{4}	1.534×10^{-3}	1.473×10^{-3}	6.064×10^{-5}
	8	2.338×10^{-2}	1.151×10^{-2}	9.385×10^{4}	1.408×10^{5}	3.973×10^{-4}	3.893×10^{-4}	7.992×10^{-6}
	9	1.170×10^{-2}	5.806×10^{-3}	7.308×10^{5}	1.096×10^{6}	1.011×10^{-4}	1.001×10^{-4}	1.026×10^{-6}
	10	5.855×10^{-3}	2.916×10^{-3}	5.767×10^{6}	8.651×10^{6}	2.551×10^{-5}	2.538×10^{-5}	1.300×10^{-7}
	11	2.929×10^{-3}	1.461×10^{-3}	4.583×10^{7}	6.875×10^{7}	6.408×10^{-6}	6.392×10^{-6}	1.636×10^{-8}
	12	1.465×10^{-3}	7.316×10^{-4}	3.652×10^{8}	5.477×10^{8}	1.606×10^{-6}	1.604×10^{-6}	2.054×10^{-9}
	13	7.324×10^{-4}	3.660×10^{-4}	2.925×10^{9}	4.388×10^{9}	4.019×10^{-7}	4.016×10^{-7}	2.564×10^{-10}
	14	3.662×10^{-4}	1.831×10^{-4}	2.347×10^{10}	3.522×10^{10}	1.005×10^{-7}	1.005×10^{-7}	3.196×10^{-11}
	15	1.831×10^{-4}	9.154×10^{-5}	1.926×10^{11}	2.899×10^{11}	2.514×10^{-8}	2.513×10^{-8}	3.894×10^{-12}
	16	9.157×10^{-5}	4.578×10^{-5}	1.629×10^{12}	2.465×10^{12}	6.286×10^{-9}	6.285×10^{-9}	4.606×10^{-13}

Table 8. Unit-variance Hui-Neuhoff pdf $p(x)=\dfrac{C_\delta}{(|x|+2)^3(\ln(|x|+2))^{\delta+1}}$, $\delta=2.38636$, $C_\delta=3.46458$

	R	x_2	y_1	x_K	y_K	D_t	D_i	D_o
Q_N^U	1		4.907×10^{-1}	0.000×10^{0}	4.907×10^{-1}	7.592×10^{-1}	0.000×10^{0}	7.592×10^{-1}
	2	9.739×10^{-1}	4.870×10^{-1}	9.739×10^{-1}	1.461×10^{0}	5.227×10^{-1}	8.795×10^{-2}	4.348×10^{-1}
	3	8.665×10^{-1}	4.333×10^{-1}	2.600×10^{0}	3.033×10^{0}	3.569×10^{-1}	7.448×10^{-2}	2.824×10^{-1}
	4	7.439×10^{-1}	3.720×10^{-1}	5.207×10^{0}	5.579×10^{0}	2.471×10^{-1}	5.362×10^{-2}	1.935×10^{-1}
	5	6.306×10^{-1}	3.153×10^{-1}	9.459×10^{0}	9.775×10^{0}	1.748×10^{-1}	3.733×10^{-2}	1.375×10^{-1}
	6	5.331×10^{-1}	2.665×10^{-1}	1.652×10^{1}	1.679×10^{1}	1.266×10^{-1}	2.594×10^{-2}	1.007×10^{-1}
	7	4.516×10^{-1}	2.258×10^{-1}	2.845×10^{1}	2.867×10^{1}	9.396×10^{-2}	1.820×10^{-2}	7.575×10^{-2}
	8	3.845×10^{-1}	1.922×10^{-1}	4.883×10^{1}	4.902×10^{1}	7.131×10^{-2}	1.297×10^{-2}	5.834×10^{-2}
	9	3.295×10^{-1}	1.648×10^{-1}	8.402×10^{1}	8.419×10^{1}	5.527×10^{-2}	9.409×10^{-3}	4.586×10^{-2}
	10	2.845×10^{-1}	1.422×10^{-1}	1.454×10^{2}	1.455×10^{2}	4.366×10^{-2}	6.948×10^{-3}	3.671×10^{-2}
	11	2.475×10^{-1}	1.237×10^{-1}	2.532×10^{2}	2.533×10^{2}	3.508×10^{-2}	5.222×10^{-3}	2.986×10^{-2}
	12	2.169×10^{-1}	1.084×10^{-1}	4.440×10^{2}	4.441×10^{2}	2.862×10^{-2}	3.991×10^{-3}	2.462×10^{-2}
	13	1.915×10^{-1}	9.573×10^{-2}	7.840×10^{2}	7.841×10^{2}	2.366×10^{-2}	3.098×10^{-3}	2.056×10^{-2}
	14	1.701×10^{-1}	8.507×10^{-2}	1.394×10^{3}	1.394×10^{3}	1.980×10^{-2}	2.439×10^{-3}	1.736×10^{-2}
	15	1.521×10^{-1}	7.607×10^{-2}	2.493×10^{3}	2.493×10^{3}	1.674×10^{-2}	1.946×10^{-3}	1.480×10^{-2}
	16	1.368×10^{-1}	6.842×10^{-2}	4.484×10^{3}	4.484×10^{3}	1.430×10^{-2}	1.572×10^{-3}	1.272×10^{-2}
	17	1.237×10^{-1}	6.186×10^{-2}	8.108×10^{3}	8.108×10^{3}	1.231×10^{-2}	1.283×10^{-3}	1.103×10^{-2}
	18	1.124×10^{-1}	5.620×10^{-2}	1.473×10^{4}	1.473×10^{4}	1.069×10^{-2}	1.058×10^{-3}	9.630×10^{-3}
	19	1.026×10^{-1}	5.129×10^{-2}	2.689×10^{4}	2.689×10^{4}	9.343×10^{-3}	8.806×10^{-4}	8.462×10^{-3}
	20	9.401×10^{-2}	4.701×10^{-2}	4.929×10^{4}	4.929×10^{4}	8.220×10^{-3}	7.390×10^{-4}	7.481×10^{-3}
Q_N^*	1		4.907×10^{-1}	0.000×10^{0}	4.907×10^{-1}	7.592×10^{-1}	0.000×10^{0}	7.592×10^{-1}
	2	1.660×10^{0}	3.591×10^{-1}	1.660×10^{0}	2.960×10^{0}	4.341×10^{-1}	1.193×10^{-1}	3.148×10^{-1}
	3	7.571×10^{-1}	2.436×10^{-1}	9.678×10^{0}	1.536×10^{1}	2.164×10^{-1}	1.023×10^{-1}	1.141×10^{-1}
	4	3.956×10^{-1}	1.549×10^{-1}	9.937×10^{1}	1.624×10^{2}	9.552×10^{-2}	5.835×10^{-2}	3.717×10^{-2}
	5	2.149×10^{-1}	9.373×10^{-2}	5.005×10^{3}	8.709×10^{3}	3.816×10^{-2}	2.690×10^{-2}	1.126×10^{-2}
	6	1.180×10^{-1}	5.467×10^{-2}	4.909×10^{6}	8.989×10^{6}	1.410×10^{-2}	1.085×10^{-2}	3.255×10^{-3}
	7	6.476×10^{-2}	3.104×10^{-2}	8.337×10^{11}	1.580×10^{12}	4.909×10^{-3}	3.995×10^{-3}	9.141×10^{-4}
	8	3.537×10^{-2}	1.728×10^{-2}	1.103×10^{21}	2.137×10^{21}	1.630×10^{-3}	1.379×10^{-3}	2.515×10^{-4}
	9	1.919×10^{-2}	9.474×10^{-3}	9.587×10^{36}	1.881×10^{37}	5.213×10^{-4}	4.532×10^{-4}	6.810×10^{-5}
	10	1.033×10^{-2}	5.131×10^{-3}	8.644×10^{64}	1.710×10^{65}	1.617×10^{-4}	1.435×10^{-4}	1.818×10^{-5}
	11	5.522×10^{-3}	2.751×10^{-3}	1.498×10^{114}	2.977×10^{114}	4.887×10^{-5}	4.408×10^{-5}	4.794×10^{-6}